Journal of Achievements in Materials and Manufacturing Engineering
VOLUME 44
ISSUE 2
February
2011

Structure, thermal and magnetic properties of $(Fe_{72}B_{20}Si_4Nb_4)_{100-x}Y_x$ (x=0.3) metallic glasses

R. Babilas*, S. Griner, P. Sakiewicz, R. Nowosielski
Institute of Engineering Materials and Biomaterials, Silesian University of Technology, ul. Konarskiego 18a, 44-100 Gliwice, Poland
* Corresponding author: E-mail address: rafal.babilas@polsl.pl

Received 13.12.2010; published in revised form 01.02.2011

Materials

ABSTRACT

Purpose: The work presents structure characterization, thermal and soft magnetic properties analysis of selected Fe-based metallic glasses in as-cast state and after crystallization process.
Design/methodology/approach: The studies were performed on $Fe_{72}B_{20}Si_4Nb_4$ and $Fe_{70}B_{19}Si_4Nb_4Y_3$ metallic glasses in form of ribbon. The amorphous structure of tested samples was examined by X-ray diffraction (XRD) and transmission electron microscopy (TEM) methods. The crystallization behaviour of the studied alloys was examined by differential thermal analysis (DTA) and differential scanning calorimetry (DSC). The soft magnetic properties examination of tested materials contained initial magnetic permeability and magnetic permeability relaxation measurements.
Findings: The XRD and TEM investigations confirmed that the studied alloys $Fe_{72}B_{20}Si_4Nb_4$ and $Fe_{70}B_{19}Si_4Nb_4Y_3$ were amorphous in as-cast state. The liquidus temperature assumed as the end temperature of the melting isotherm on the DTA reached a value of 1550 K and 1560 K for $Fe_{72}B_{20}Si_4Nb_4$ and $Fe_{70}B_{19}Si_4Nb_4Y_3$ alloy, adequately. The analysis of crystallization process indicated that onset and peak crystallization temperature increased with increasing of heating rate at DSC measurements. The samples of $Fe_{72}B_{20}Si_4Nb_4$ alloy presented two stage crystallization process. The initial magnetic permeability of examined samples increased together with the increase of annealing temperature and reached a distinct maximum at 773 K for $Fe_{72}B_{20}Si_4Nb_4$ and at 723 K for $Fe_{70}B_{19}Si_4Nb_4Y_3$ alloy.
Practical implications: The increasing of annealing temperature significantly improved soft magnetic properties of examined alloys by increase the initial magnetic permeability.
Originality/value: The applied investigation methods are suitable to determine the changes of structure and selected properties between studied alloys, especially in aspect of the soft magnetic properties improvement after annealing process.
Keywords: Materials; Amorphous materials; Metallic glasses; Thermal stability; Soft magnetic properties

Reference to this paper should be given in the following way:
R. Babilas, S. Griner, P. Sakiewicz, R. Nowosielski, Structure, thermal and magnetic properties of $(Fe_{72}B_{20}Si_4Nb_4)_{100-x}Y_x$ (x=0.3) metallic glasses, Journal of Achievements in Materials and Manufacturing Engineering 44/2 (2011) 140-147.

1. Introduction

Metallic glasses (MGs) constitute a novel and important class of metallic materials with good physical and mechanical properties, that can be exploited for many applications [1-3]. Iron-based metallic glasses have received great attention of researchers, because of their good soft magnetic properties and candidates as precursors for nanocrystalline materials [4,5].

In the cases of Fe-based metallic glasses Inoue et al. succeeded in achieving a number of metallic glasses such as Fe-(Al, Ga)-P-C-B, Fe-(Co, Ni)-(Zr, Hf, Nb, Ta)-B, Fe-(Cr,Mo)-B-C, Fe-(Co,Ni)-B-Si-Nb and Fe-B-Si-Nb alloys. These systems alloys have good glass-forming ability and could be prepared in different bulk forms with low critical cooling rates [6].

The Fe-based metallic glasses with good glass-forming ability (GFA) should realized the empirical rules proposed by Inoue. These rules said that alloy with good GFA: (1) should have at least three components, two of which are metallic; (2) the alloy should contain two or more metallic elements with different atomic sizes and near-zero heats of mixing; (3) the metallic elements should have large negative heats of mixing with the metalloid type of components [7].

In addition to GFA empirical rules, it has been reported that a small addition of Y in multi-component Fe-based glassy alloys improved the GFA. The effect of Y on glass formation was considered by scavenging the oxygen impurity from alloy and adjusting the compositions closer to the eutectic and decreasing their liquidus temperature [8,9].

The work was succeeded in fabrication of $Fe_{72}B_{20}Si_4Nb_4$ and $Fe_{70}B_{19}Si_4Nb_4Y_3$ metallic glasses, which are classified for the Fe-based bulk amorphous alloy systems proposed by Inoue. This alloys seem to have good glass-forming ability, great thermal stability and good soft magnetic properties. Additionally, this paper intends to compare these alloys and presents the effect of substitution of Y for Fe on the thermal and magnetic properties.

2. Material and research methodology

The aim of this paper is the structure characterization, thermal stability and soft magnetic properties analysis of $(Fe_{72}B_{20}Si_4Nb_4)_{100-x}Y_x$ (x = 0, 3) amorphous alloy system in as-cast state and after heat treatment processing. Investigations were done with use of XRD, TEM, DTA, DSC and magnetic measurements methods.

The investigated material was cast in form of the ribbons. The ingot was prepared by induction melting of a mixture of pure elements of Fe, Nb, Y and ferroalloys Fe-B, Fe-Si under protective gas atmosphere.

The investigated materials were cast as ribbon shaped metallic glasses with thickness (*g*) 0.03 mm and width (*d*) 10 mm. The ribbons were manufactured by the "chill-block melt spinning" (CBMS) technique (Fig. 1), which is a method of continuous casting of the liquid alloy on the surface of a turning copper based wheel [10-19].

In order to study crystallization processes, ribbons in the as-cast state were annealed at the temperature range from 873 K to 923 K. Tested samples were annealed in electric chamber furnace under protective argon atmosphere. The annealing time was constant and equaled to 1 hour.

Structure analysis of the samples was carried out using X-ray diffractometer (XRD) with $Co_{K\alpha}$ radiation. The data of diffraction lines were recorded by "step-scanning" method in 2θ range from 30° to 90° for samples in as-cast state and from 35° to 90° for annealed ribbons.

Transmission electron microscopy (TEM) was used for the structural characterization of ribbons in as-cast state and after annealing procedure. Thin foils for TEM observation (from central part of tested samples) were prepared by an electrolytic polishing method after previous mechanical grinding.

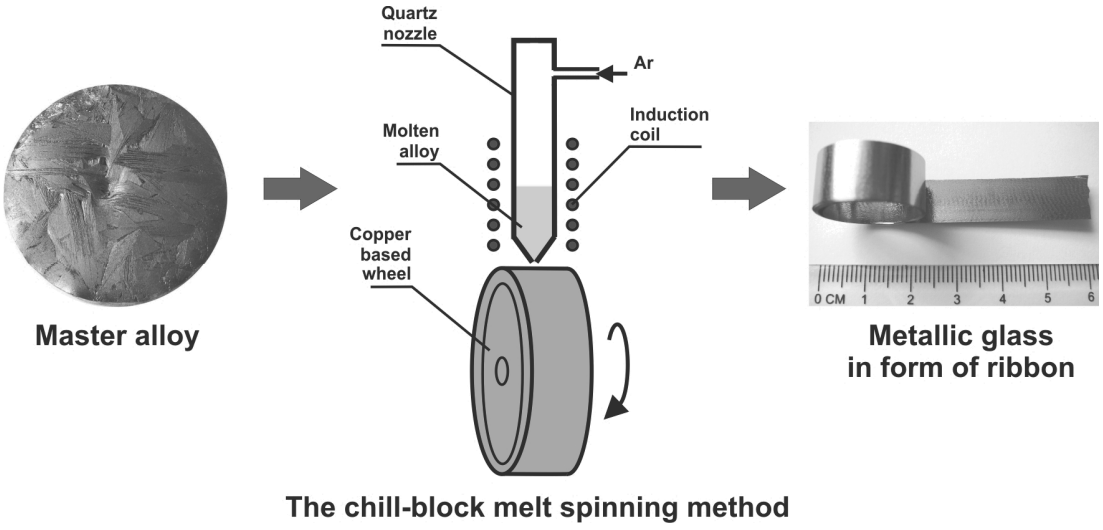

Fig. 1. Schematic illustration of the chill-block melt spinning method used for amorphous ribbons casting

The liquidus temperature of master alloys were measured using the differential thermal analysis (DTA) at a constant heating rate of 6 K/s under an argon protective atmosphere.

Thermal stability associated with onset (T_x) and peak (T_p) crystallization temperatures was examined by differential scanning calorimetry (DSC). The heating rate of calorimetry measurements, under an argon protective atmosphere, was 5 K/min and 20 K/min for comparison.

Magnetic measurements of annealed ribbons of studied alloys, carried at room temperature, included following properties:

a) relative magnetic permeability (μ_r) - determined with Maxwell-Wien bridge at a frequency of 1030 Hz and magnetic field H= 0.5 A/m;
b) magnetic permeability relaxation ($\Delta\mu/\mu$) also defined as "magnetic after-effects" - determined by measuring changes of magnetic permeability as a function of time after demagnetization, where $\Delta\mu$ is difference between magnetic permeability determined at t_1 = 30 s and t_2 = 1800 s after demagnetization [20,21].

3. Results and discussion

The X-ray diffraction investigations confirmed that the studied alloys $Fe_{72}B_{20}Si_4Nb_4$ and $Fe_{70}B_{19}Si_4Nb_4Y_3$ are amorphous in as-cast state.

The diffraction pattern of the $Fe_{72}B_{20}Si_4Nb_4$ (Fig. 2) and $Fe_{70}B_{19}Si_4Nb_4Y_3$ (Fig. 3) alloy cast in form of ribbons with thickness of 0.03 mm shows the broad diffraction halo characteristic for the amorphous structure of Fe-based glassy alloys.

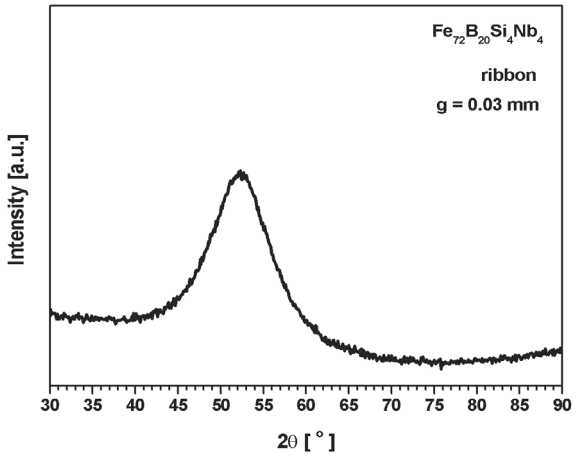

Fig. 2. X-ray diffraction patterns of $Fe_{72}B_{20}Si_4Nb_4$ glassy ribbon in as-cast state with thickness of 0.03 mm

Figures 4 and 5 show TEM images and electron diffraction patterns of studied samples in as-cast state. The TEM images reveal only a changing of contrast, which is characteristic for amorphous structure. The electron diffraction pattern consists only halo rings. Broad diffraction halo can be seen for each tested alloys, indicating the formation of a glassy phase.

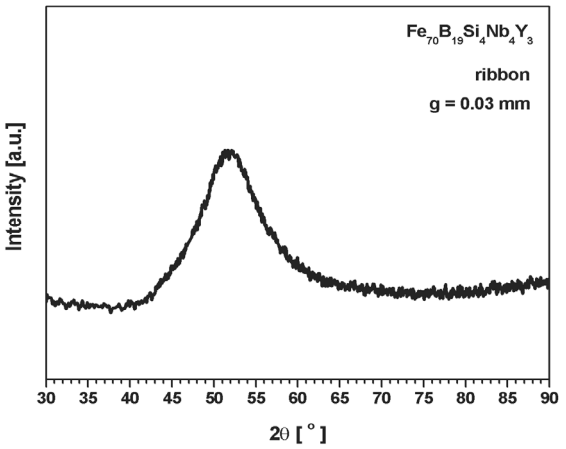

Fig. 3. X-ray diffraction patterns of $Fe_{70}B_{19}Si_4Nb_4Y_3$ glassy ribbon in as-cast state with thickness of 0.03 mm

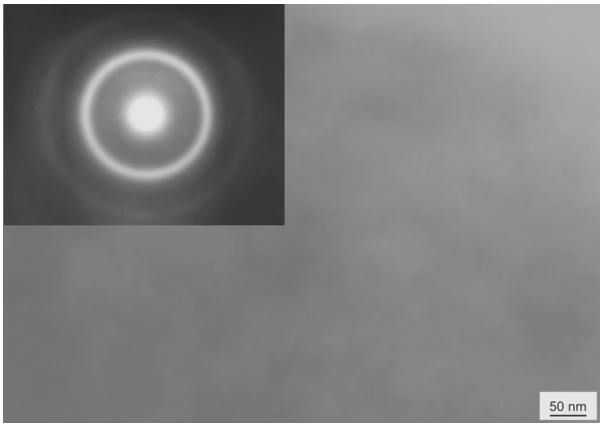

Fig. 4. Transmission electron micrograph and electron diffraction pattern of the as-cast glassy $Fe_{72}B_{20}Si_4Nb_4$ ribbon with thickness of 0.03 mm

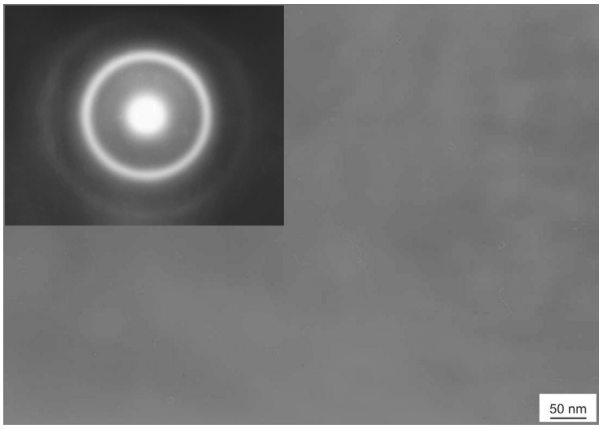

Fig. 5. Transmission electron micrograph and electron diffraction pattern of the as-cast glassy $Fe_{70}B_{19}Si_4Nb_4Y_3$ ribbon with thickness of 0.03 mm

Based from the XRD results and TEM investigations of the studied samples, it was believed that the tested amorphous alloys can be fabricated into a bulk glassy samples.

The Fe-Si-B system, as the basic for the composition of Fe-B-Si-Nb and Fe-B-Si-Nb-Y alloy realizes the empirical rules for good glass-forming ability. The addition of Nb and Y into this alloy system supports the Inoue's rules concerning multicomponent alloy systems, consisting on more than three elements. The studied alloys consists of four and five elements.

The significant difference in atomic radius among the main constituent elements is like follows: yttrium (0.17 nm) > niobium (0.147 nm) > iron (0.127 nm) > silicon (0.112 nm) > boron (0.084 nm).

The melting temperature (T_m) and liquidus temperature (T_l) assumed to be the onset and end temperature of the melting isotherm on the DTA (at 6 K/min) curves are presented in Figures 6 and 7.

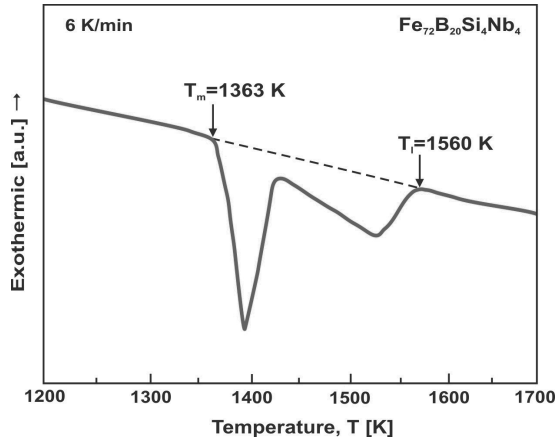

Fig. 6. DTA curve of $Fe_{72}B_{20}Si_4Nb_4$ alloy as master-alloy

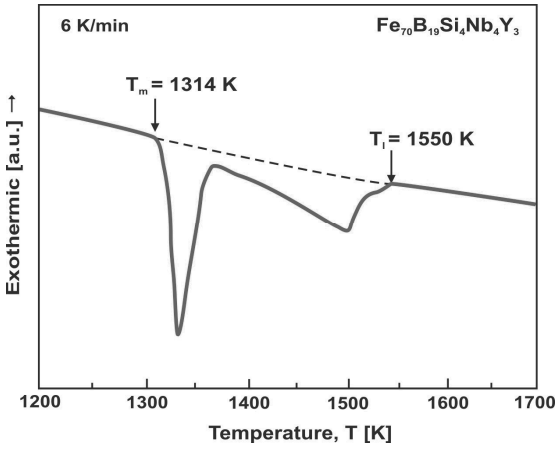

Fig. 7. DTA curve of $Fe_{70}B_{19}Si_4Nb_4Y_3$ alloy as master-alloy

The endothermic peak observed on DTA curve of master alloy of $Fe_{72}B_{20}Si_4Nb_4$ metallic glass allowed to determine the melting temperature (T_m), which has a value of 1363 K and liquidus temperature (T_l = 1560 K). In the similar way the endothermic effect was also observed for master alloy of second studied material ($Fe_{70}B_{19}Si_4Nb_4Y_3$). The melting temperature (T_m) reached a value of 1314 K and liquidus temperature (T_l) had a value of 1550 K.

In addition to DTA analysis of master alloys of studied materials Table 1 shows melting temperature (T_m) and liquidus temperature (T_l) of studied materials. The addition of Y in $Fe_{70}B_{19}Si_4Nb_4Y_3$ alloy insensibly decreases the melting and liquidus temperature in comparison to $Fe_{72}B_{20}Si_4Nb_4$ alloy.

Table 1.
Thermal properties of $Fe_{72}B_{20}Si_4Nb_4$ and $Fe_{70}B_{19}Si_4Nb_4Y_3$ master alloys

Master alloy	T_m [K]	T_l [K]
$Fe_{72}B_{20}Si_4Nb_4$	1363	1560
$Fe_{70}B_{19}Si_4Nb_4Y_3$	1314	1550

The DSC curves (at heating rates of 5 and 20 K/min) measured on amorphous ribbons of $Fe_{72}B_{20}Si_4Nb_4$ and $Fe_{70}B_{19}Si_4Nb_4Y_3$ alloys with thickness of 0.03 mm in as-cast state are shown in Figures 8 and 9.

The two exothermic peaks describing crystallization of $Fe_{72}B_{20}Si_4Nb_4$ alloy were observed for studied samples after two different heating rates. The crystallization effect for the ribbon sample after heating of 5 K/min informs about two stage crystallization process and includes onset crystallization temperature of T_x = 871 K and peak crystallization temperature of T_{p1} = 891 K and T_{p2} = 913 K. In the case of the 20 K/min heating rate, the exothermic effect includes higher values of the crystallization temperatures. After heating at 20 K/min onset crystallization temperature reaches a value of T_x = 893 K and peak crystallization temperature has a value of T_{p1} = 911 K. The second crystallization stage of studied ribbon is described by peak with temperature of T_{p2} = 924 K.

The DSC curves obtained for ribbons of $Fe_{70}B_{19}Si_4Nb_4Y_3$ alloy informs about the single stage of crystallization process. The onset crystallization temperature after heating at 5 K/min has a value of T_x = 839 K and peak crystallization temperature reaches a value of T_p = 856 K. The analysis of the crystallization process after higher heating rate (20 K/min) gives also information about higher temperatures in comparison to 5 K/min. The onset and peak crystallization temperature of examined ribbons has a value of 854 and 873 K, adequately. The analysis of crystallization process of examined alloys shows that onset and peak crystallization temperature increases with increasing of heating rate. What is more, the samples of $Fe_{72}B_{20}Si_4Nb_4$ alloy presented two stage crystallization process.

The thermal stability parameters of studied glasses - onset crystallization temperature (T_x) and peak crystallization temperature (T_p) are presented in Table 2.

Figures 10 and 11 show X-ray diffraction patterns obtained for $Fe_{70}B_{19}Si_4Nb_4Y_3$ alloy in form of ribbon with thickness of 0.03 mm after annealing at 873 and 923 K for 1 hour.

The annealing process realized at mention temperatures obviously causes formation of crystalline phases. The structure after annealing at 873 K for 1 hour, corresponding to the temperature of the exothermic peak determined after DSC examination at 20 K/m heating rate, consisted a mixture of FeB, Fe_2B, Fe_3B and α-Fe phases.

Table 2.
Thermal properties of the studied alloys in forms of glassy ribbons, in as-cast state

Glassy alloy	Heating rate [K/min]	T_x [K]	T_{p1} [K]	T_{p2} [K]
$Fe_{72}B_{20}Si_4Nb_4$	5	871	891	913
	20	893	911	924
$Fe_{70}B_{19}Si_4Nb_4Y_3$	5	839	856	-
	20	854	873	-

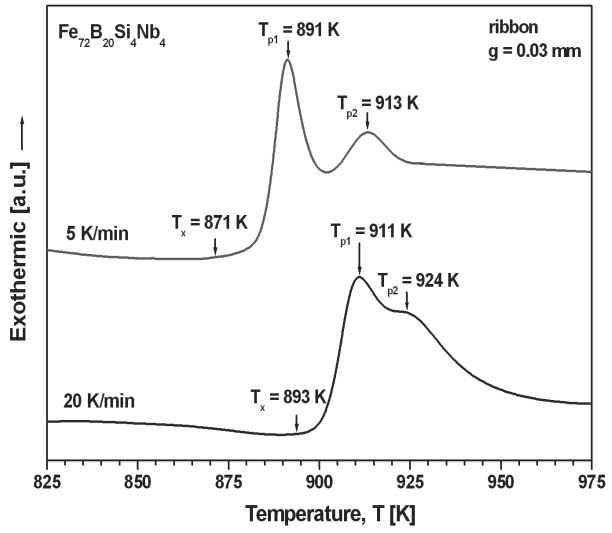

Fig. 8. DSC curves of $Fe_{72}B_{20}Si_4Nb_4$ glassy alloy ribbons in as-cast state (heating rate 5 and 20 K/min)

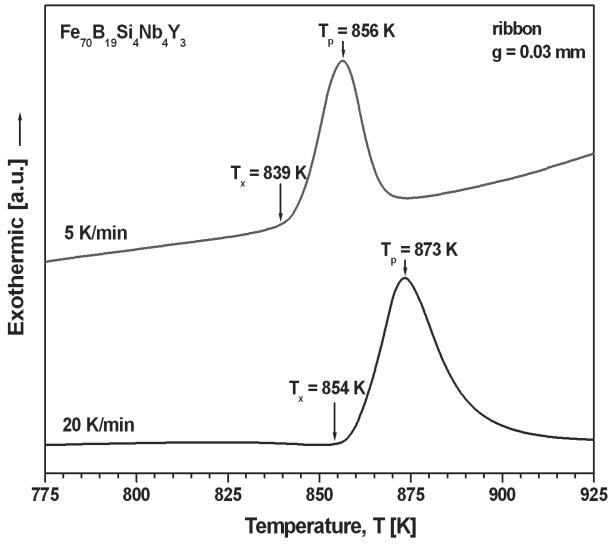

Fig. 9. DSC curves of $Fe_{70}B_{19}Si_4Nb_4Y_3$ glassy alloy ribbons in as-cast state (heating rate 5 and 20 K/min)

Qualitative phase analysis from X-ray data of examined ribbons annealed at 923 K enables also the identification of α-Fe phase and borides FeB, Fe_2B and Fe_3B.

It is noticed, that annealing process in studied temperature range leads to a formation of many crystalline phases, which quantity increases with increasing of annealing temperature. Comparison of diffraction patterns of $Fe_{70}B_{19}Si_4Nb_4Y_3$ alloy after annealing from 873 K to 923 K also shows the increasing of diffraction lines intensity.

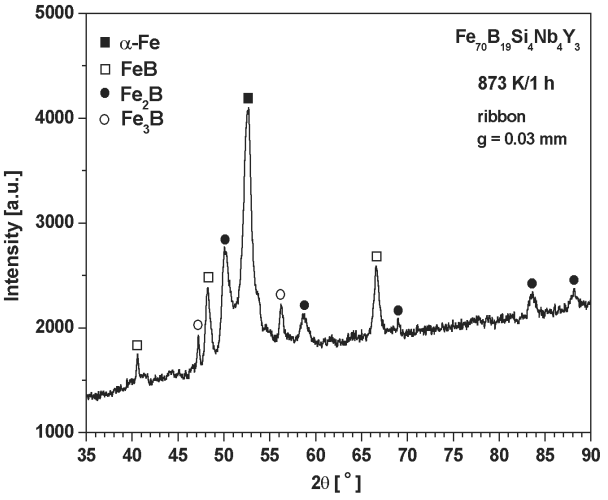

Fig. 10. X-ray diffraction patterns of $Fe_{70}B_{19}Si_4Nb_4Y_3$ alloy (ribbon with thickness of 0.03 mm) after annealing at 873 K for 1 hour

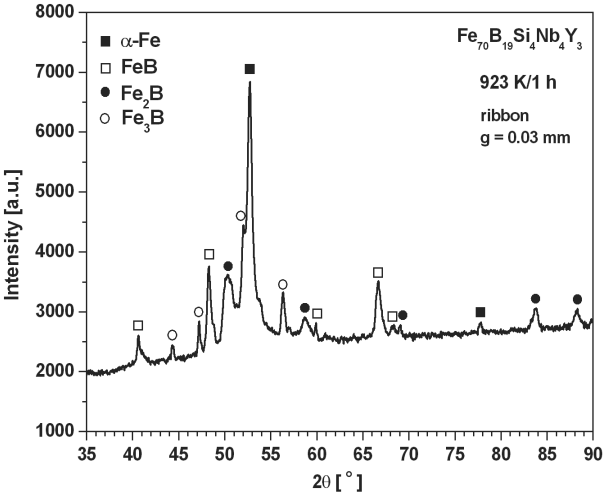

Fig. 11. X-ray diffraction patterns of $Fe_{70}B_{19}Si_4Nb_4Y_3$ alloy (ribbon with thickness of 0.03 mm) after annealing at 923 K for 1 hour

The crystallization process of $Fe_{72}B_{20}Si_4Nb_4$ alloy determined by XRD and TEM methods was describing in detail in works [10-12] published by author.

a) b)

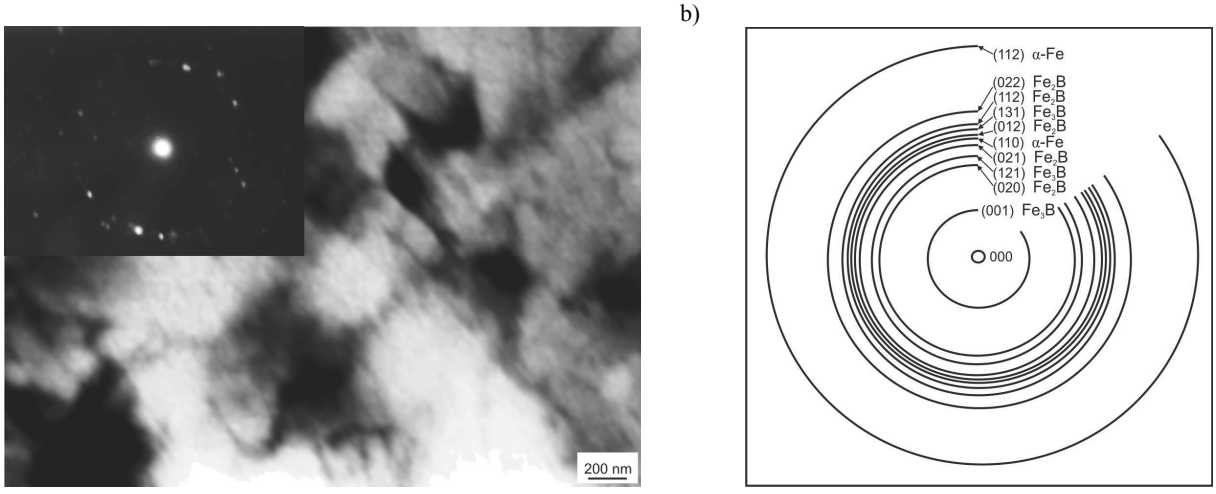

Fig. 12. Transmission electron micrograph plus electron diffraction pattern (a) and the solution of diffraction pattern (b) of $Fe_{70}B_{19}Si_4Nb_4Y_3$ alloy in form of ribbon (g = 0.03 mm) after annealing at 873 K for 1 hour

a) b)

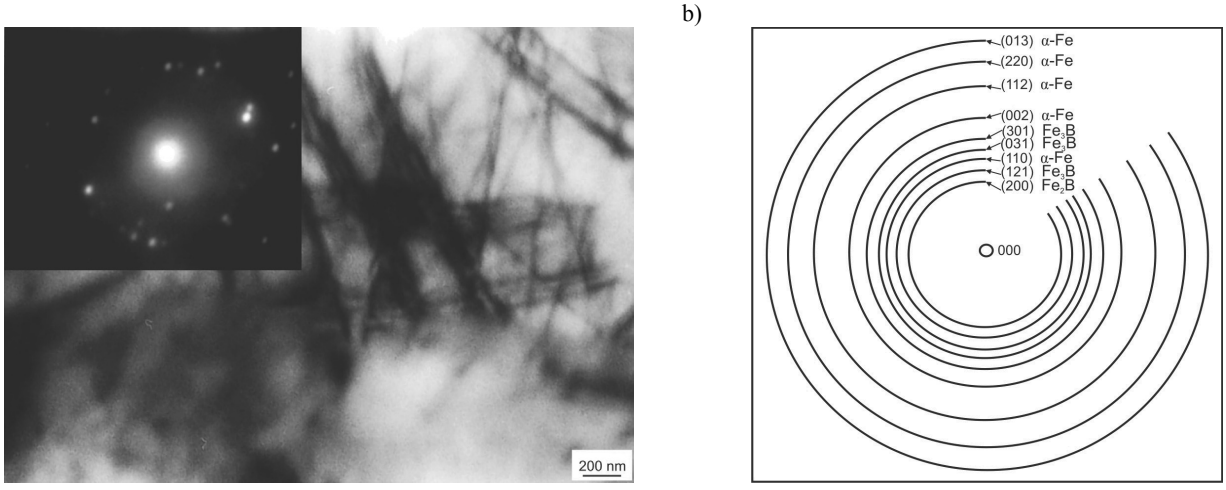

Fig. 13. Transmission electron micrograph plus electron diffraction pattern (a) and the solution of diffraction pattern (b) of $Fe_{70}B_{19}Si_4Nb_4Y_3$ alloy in form of ribbon (g = 0.03 mm) after annealing at 923 K for 1 hour

The TEM examinations confirmed the formation of the crystals in samples of $Fe_{70}B_{19}Si_4Nb_4Y_3$ alloy after annealing at temperature of 873 and 923 K. Figures 12 and 13 show the transmission electron micrographs plus electron diffraction patterns and their solutions obtained for ribbons of studied alloy after annealing at mentioned temperatures for 1 hour.

The annealing process in temperature range from 873 K to 923 K obviously causes formation of the crystalline phases. The phase analysis performed from the electron diffraction patterns of $Fe_{70}B_{19}Si_4Nb_4Y_3$ alloy enables the identification of α-Fe phase and iron borides – Fe_2B and Fe_3B.

The initial magnetic permeability (μ_r) for ribbons with thickness of 0.03 mm for both examined alloys determined at room temperature versus annealing temperature (T_a) is shown in Figure 14. The initial magnetic permeability of the examined samples increases together with the increase of annealing temperature and reaches a distinct maximum at 773 K for $Fe_{72}B_{20}Si_4Nb_4$ and at 723 K for $Fe_{70}B_{19}Si_4Nb_4Y_3$ alloy. The temperature of annealing process, which corresponds to the maximum of initial magnetic permeability (μ_{rmax} = 2550 for $Fe_{72}B_{20}Si_4Nb_4$ and μ_{rmax} = 1330 for $Fe_{70}B_{19}Si_4Nb_4Y_3$) may be defined as the optimization of the annealing temperature (T_{op}) of studied alloys.

Magnetic permeability relaxation (defined as magnetic after-effects) for tested ribbons was determined as well. The $\Delta\mu/\mu$ is directly proportional to the concentration of defects in amorphous materials, i.e. free volume concentration [20,21]. The value of $\Delta\mu/\mu$ determined at the optimization of the annealing temperature of tested alloys is of 1.7 and 2.3 % for ribbons of $Fe_{72}B_{20}Si_4Nb_4$ and $Fe_{70}B_{19}Si_4Nb_4Y_3$ alloy, adequately.

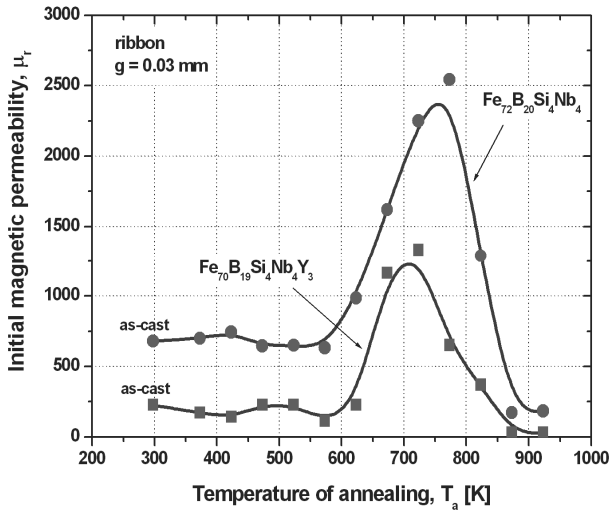

Fig. 14. Initial magnetic permeability of $Fe_{72}B_{20}Si_4Nb_4$ and $Fe_{70}B_{19}Si_4Nb_4Y_3$ alloy in form of ribbons, determined at room temperature versus annealing temperature

The small addition of Y (3 at.%) in $Fe_{72}B_{20}Si_4Nb_4$ alloy improved thermal properties (by decreasing the melting and liquidus temperature), but it also decreased the initial magnetic permeability of examined material.

Table 3 summarises information concerning magnetic properties of the studied alloys in form of the ribbons with thickness of 0.03 mm after annealing at optimized temperature (T_{op}).

Table 3.
Magnetic properties of studied alloys after annealing at optimized temperature (T_{op})

Alloy	g [mm]	T_{op} [K]	μ_r	$\Delta\mu/\mu$ [%]
$Fe_{72}B_{20}Si_4Nb_4$	0.03	773	2550	1.7
$Fe_{70}B_{19}Si_4Nb_4Y_3$		723	1330	2.3

4. Conclusions

The investigations performed on the samples of the $Fe_{72}B_{20}Si_4Nb_4$ and $Fe_{70}B_{19}Si_4Nb_4Y_3$ metallic glasses allowed to formulate the following statements:

- the XRD and TEM investigations revealed that the studied alloys $Fe_{72}B_{20}Si_4Nb_4$ and $Fe_{70}B_{19}Si_4Nb_4Y_3$ (in form of ribbons) were amorphous in as-cast state.
- the liquidus temperature (T_l) assumed as the end temperature of the melting isotherm on the DTA reached a value of 1550 K and 1560 K for $Fe_{72}B_{20}Si_4Nb_4$ and $Fe_{70}B_{19}Si_4Nb_4Y_3$, adequately,
- the analysis of crystallization process of examined alloys indicated that onset and peak crystallization temperature increases with increasing of heating rate (5-20 K/min),
- the samples of $Fe_{72}B_{20}Si_4Nb_4$ alloy presented two stage crystallization process, but addition of Y caused single stage crystallization behavior,
- the annealing treatment caused the formation of the α-Fe and iron borides crystalline phases,
- the initial magnetic permeability of the examined samples increased together with the increase of annealing temperature and reached a distinct maximum at 773 K for $Fe_{72}B_{20}Si_4Nb_4$ and at 723 K for $Fe_{70}B_{19}Si_4Nb_4Y_3$ alloy,
- the $\Delta\mu/\mu$ determined at the optimization of the annealing temperature of tested alloys had a value of 1.7 and 2.3 % for ribbons of $Fe_{72}B_{20}Si_4Nb_4$ and $Fe_{70}B_{19}Si_4Nb_4Y_3$ alloy, adequately,
- the addition of Y into Fe-B-Si-Nb alloy insensibly decreased the melting temperature of it, but also decreased the initial magnetic permeability.

Acknowledgements

The authors would like to thank Dr A. Zajączkowski (Non-Ferrous Metals Institute, Gliwice), Dr T. Czeppe (Institute of Metallurgy and Materials Science, Kraków) and Dr Z. Stokłosa (Institute of Materials Science, University of Silesia, Katowice) for a cooperation and helpful comments.

This work was supported by Polish Ministry of Science (grant N507 027 31/0661).

References

[1] A. Inoue, K. Hashimoto, Amorphous and nanocrystalline materials: preparation, properties and applications, Springer, 2001.
[2] R. Hasegawa, Glassy metals: magnetic, chemical and structural properties, CRC Press, Florida, 2000.
[3] L.A. Dobrzański, M. Drak, B. Ziębowicz, Materials with specific magnetic properties, Journal of Achievements in Materials and Manufacturing Engineering 17/1-2 (2006) 37-40.
[4] T. Kulik, Nanocrystallization of metallic glasses, Journal of Non-Crystalline Solids 287 (2001) 145-161.
[5] B. Ziębowicz, M. Drak, L.A. Dobrzański, Corrosion resistance of the composite materials: nanocrystalline powder – polymer type in acid environment, Journal of Achievements in Materials and Manufacturing Engineering 36/2 (2009) 126-133.
[6] A. Inoue, Stabilization of supercooled liquid and opening-up of bulk glassy alloys, Proceedings of the Japan Academy 73 B (1997) 19-24.
[7] A. Inoue, A. Makino, T. Mizushima, Ferromagnetic bulk glassy alloys, Journal of Magnetism and Magnetic Materials 215-216 (2000) 246-252.
[8] D.S. Song, J.H. Kim, E. Fleury, W.T. Kim, D.H. Kim, Synthesis of ferromagnetic Fe-based bulk glassy alloys in the Fe-Nb-B-Y system, Journal of Alloys and Compounds 389 (2005) 159-164.

[9] J. Zhang, H. Tan, Y.P. Feng, Y. Li, The effect of Y on glass forming ability, Scripta Materialia 53 (2005) 183-187.
[10] R. Nowosielski, R. Babilas, S. Griner, G. Dercz, A. Hanc, Crystallization of $Fe_{72}B_{20}Si_4Nb_4$ metallic glasses ribbons, Journal of Achievements in Materials and Manufacturing Engineering 34/1 (2009) 15-22.
[11] R. Nowosielski, R. Babilas, Structure and properties of selected Fe-based metallic glasses, Journal of Achievements in Materials and Manufacturing Engineering 37/2 (2009) 332-339.
[12] R. Babilas, R. Nowosielski, Iron-based bulk amorphous alloys, Archives of Materials Science and Engineering, 44/1 (2010) 5-27.
[13] J. Konieczny, L.A. Dobrzański, J.E. Frąckowiak, Structure and properties of the powder obtained from the amorphous ribbon, Journal of Achievements in Materials and Manufacturing Engineering 18/1-2 (2006) 143-146.
[14] D. Szewieczek, T. Raszka, Structure and magnetic properties of $Fe_{63.5}Co_{10}Cu_1Nb_3Si_{13.5}B_9$ alloy, Journal of Achievements in Materials and Manufacturing Engineering 18 (2006) 179-182.
[15] D. Szewieczek, T. Raszka, Influence of Na_2SO_4 on magnetic properties of $(Fe_{1-x}Co_x)_{73.5}Cu_1Nb_3Si_{13.5}B_9$ (x = 10,40) alloys, Journal of Achievements in Materials and Manufacturing Engineering 17/1-2 (2006) 161-164.
[16] D. Szewieczek, T. Raszka, J. Olszewski, Optimisation the magnetic properties of the $(Fe_{1-x}Co_x)_{73.5}Cu_1Nb_3Si_{13.5}B_9$ (x = 10; 30; 40) alloys, Journal of Achievements in Materials and Manufacturing Engineering 20 (2007) 31-36.
[17] S. Lesz, D. Szewieczek, J.E. Frąckowiak, Structure and magnetic properties of amorphous and nanocrystalline $Fe_{85.4}Hf_{1.4}B_{13.2}$ alloy, Journal of Achievements in Materials and Manufacturing Engineering 19/2 (2006) 29-34.
[18] D. Szewieczek, J. Tyrlik-Held, S. Lesz, Structure and mechanical properties of amorphous $Fe_{84}Nb_7B_9$ alloy during crystallization, Journal of Achievements in Materials and Manufacturing Engineering 24/2 (2007) 87-90.
[19] S. Lesz, D. Szewieczek, J. Tyrlik-Held, Correlation between fracture morphology and mechanical properties of NANOPERM alloys, Archives of Materials Science and Engineering 29/2 (2008) 73-80.
[20] P. Kwapuliński, J. Rasek, Z. Stokłosa, G. Badura, B. Kostrubiec, G. Haneczok, Magnetic and mechanical properties in FeXSiB (X = Cu, Zr, Co) amorphous alloys, Archives of Materials Science and Engineering 31/1 (2008) 25-28.
[21] P. Kwapuliński, Z. Stokłosa, J. Rasek, G. Badura, G. Haneczok, L. Pająk, L. Lelątko, Influence of alloying additions and annealing time on magnetic properties in amorphous alloys based on iron, Journal of Magnetism and Magnetic Materials 320 (2008) 778-782.